Evolutionary synthesis models for spirals and irregular galaxies

Mercedes Mollá

CIEMAT, Avda. Complutense 22, 28040, Madrid mercedes.molla@ciemat.es

Summary. We show autoconsistent chemical and spectro-photometric evolution models applied to spiral and irregular galaxies. Evolutionary synthesis models usually used to explain the stellar component spectro-photometric data, are combined with chemical evolution models, to determine precisely the evolutionary history of spiral and irregular galaxies. In this piece of work we will show the results obtained for a wide grid of modeled theoretical galaxies.

1 Introduction

It is well known that galaxies have different spectral energy distributions (SEDs) depending on their morphological type [2]. These SEDs, and other data related to the stellar phase, are usually analysed through (evolutionary) synthesis models (see [5, 7] for a recent and updated review about these models), based on single stellar populations (SSPs), created by an instantaneous burst of star formation (SF). These codes compute the SED, S_λ, and the corresponding colors, surface brightness and/or spectral absorption indices emitted by a SSP of metallicity Z and age τ, from the sum of spectra of all stars created and distributed along a HR diagram, convolved with an initial mass function. This SED, given τ and Z, is characteristic of each SSP.

SF, however, does not always take place in a single burst, as occurs in spiral and irregular galaxies where star formation is continuous or in successive bursts. In that case, the characteristic τ and Z found after fitting a SSP model to an observed SED represent only averaged values, leading to a loss of information. Our aim is to obtain the time evolution of the galaxy, given by the SF history (SFH) and the age-metallicity relation (AMR). When more than a single generation of stars exists in a region or galaxy, the final SED, F_λ, corresponds to the light emitted by successive generations of stars. It may be calculated as the sum of several SSP SEDs, S_λ, being weighthed by the created stellar mass in each time step,implying a convolution with the SFH, $\Psi(t)$:

$$F_\lambda(t) = \int_0^t S_\lambda(\tau, Z)\Psi(t')dt', \tag{1}$$

where $\tau = t - t'$.

This requires to us make hypotheses about the shape and the intensity of the SFH, e.g. an exponentially decreasing function of time is usually assumed. The fit will give the best parameters that are needed to define the assumed function. In fact, in order to avoid bias, one would need to consider also other possible SFHs and their parameters fits, but computational resources precluded the study of such large model grids. Moreover. an important point, usually forgotten when this technique is applied, is that $S_\lambda(\tau, Z) = S_\lambda(\tau, Z(t'))$, that is, the metallicity changes with time since stars form and die continously. It is not clear which Z must be selected at each time step without knowing this function $Z(t)$. Usually, only one Z is used for the whole integration which may be an over-simplification.

A better method ([1]) is to perform a least square technique to find the best superposition of these SSP's which will fit the data. This gives the proportions of stellar mass created at a given metallicity and age that better reproduce observations, thus providing the SFH, $\Psi(t)$, and the AMR, $Z(t)$, as results. This technique, although essentially correct, produces, at the moment, poor evolutionary histories, having low time resolution due to large bin widths.

In summary, it is clear that spiral and irregular galaxies are systems more complex than those represented by SSP's, and that, in particular, their chemical evolution must be taken into account for a precise interpretation of the spectrophotometric data. On the plus side for these objects the gas phase data are also available and may be used as constraint. What is required then is to determine the possible evolutionary paths followed by a galaxy that arrive at the observed present state, while, simultaneously, reproducing the average photometric properties defined by the possible subjacent stellar populations.

2 Chemical evolution models

The information coming from the gas phase, such as density, abundance, and actual star formation rate, is usually analysed using chemical evolution models. They describe how the proportion of heavy elements present in the interstellar medium (ISM) increases, starting from primordial abundances, when stars evolve and die.

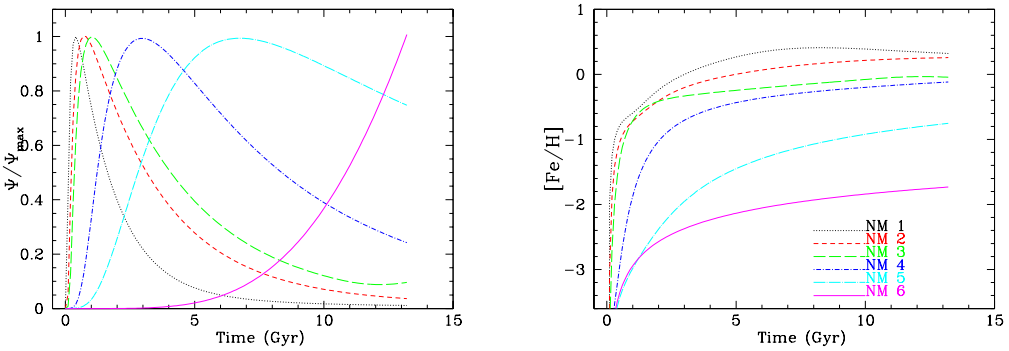

Fig. 1. The resulting SFH, $\Psi(t)$, and AMR, [Fe/H](t) for models of Table 1

Modern codes solve numerically the system of equations used to describe a scenario based on initial conditions for the total mass of the region, the existence of infall or outflow of gas, and the initial mass function (IMF). Stellar mean-lifetimes and yields, known from stellar evolutionary tracks are also included. Finally, a SF law is assumed. The *best* model for a galaxy will of course be the one which reproduces the observational data as closely as possible.

Table 1. Selected models similar to some known galaxies

Ndis	Vrot km.s^{-1}	N	R_{opt} kpc	τ_{col} Gyr	Ψ_{max} $M_\odot$.yr^{-1}	$t_{\Psi,max}$ Gyr	$[Fe/H]_p$	Galaxy	T	Type
43	371	1	29	1.65	318	0.32	0.322	M81	2	Sab
38	266	3	21	2.66	78	0.60	0.258	M31	3	Sb
28	200	4	13	4.00	32.39	1.05	-0.04	MWG	4	Sbc
18	99	6	7	11.00	2.78	3.02	-0.12	M33	6	Scd
13	87	8	4	13.3	0.20	6.68	-0.75	NGC300	7	Sdm
8	78	10	2.3	17.7	0.0013	13.2	-1.73	D0154	10	Im

We use here the multiphase chemical evolution model, described in [3, 4, 9]. We have computed in [8] a large grid of models for 44 theoretical galaxies with variable initial masses and sizes obtained with the universal rotation curve of [11]. The mass in each modeled galaxy, initially in the form of gas, is in a protohalo, from which it falls onto an equatorial plane leading to the formation of the disc. The gas infall rate, or its inverse the collapse-time scale, depends on the total mass. For each of these 44 galaxies we assumed 10 possible molecular cloud and SF efficiencies, ϵ, which may take values in the range [0,1] and which are distinguished by the number N. In this way we computed models in the whole plane [Vrot, N] (or Vrot-ϵ). Within this plane, the bright galaxies are located on the diagonal axis, where the most massive spiral galaxies are usually those of earliest morphological types [12] which, in turn, need the highest star formation efficiencies (see Fig.4 from [8]). Furthermore, there exist other well defined zones in this plane corresponding to other classes of galaxies, such as the low mass dwarf galaxies (Vrot < 70 km.s^{-1}).

This grid reproduces well the generic data trends for the normal bright spiral and irregular galaxies, in particular the radial distributions observed for the gas, the stars, the SFR and the elemental abundances in particular galaxies (see [8] for details). Each model produces the time evolution within a galaxy, that is, the resulting SFH and AMR for several radial regions. We show these evolutionary histories in Fig. 1 for the selected models given in Table 1. In this table we give the number of the mass distribution $Ndis$ and its corresponding rotation velocity $Vrot$ in columns 1 and 2, the number N which defines the SF efficiency in column 3, and the disk radius Ropt and collapse time scale τ_{col} in columns 4 and 5. The SF, as we may see in panel a) of Fig.1 has a maximum Ψ_{max} (with which we have normalized the curves of panel a)), at a given time $t_{\Psi,max}$ which is different for each model. Both values are given in columns 6 and 7 of the same table. In column 8 we give the present time Iron abundance $[Fe/H]_p$. Each one of these models is representative of a well known galaxy as those referenced in column 9, as checked in [8].

3 Evolutionary synthesis models

From the results of the above section, we take the SFH and the AMR as inputs in Eq. 1 to compute the SED of each galaxy. The set of SSP's SEDs used are those from the evolutionary synthesis code described in [10]. For each stellar generation created in the time step t', a SSP-SED, $S(\tau)$, from this set is chosen taking into account its age, $\tau = t - t'$, from the time t' in which it was created until the present t, and the metallicity $Z(t')$ reached by the gas. After convolution with the SFH, $\Psi(t)$, the final SED, $F(\lambda)$, is obtained.

The resulting F(λ) reproduce reasonably well the SEDs of galaxies such as can be seen in Fig. 2. There we compare our resulting spectra for the models of the known galaxies of Table 1 to the different morphological type templates from [2].

In order to use our model grid, we may therefore to select the best model able to fit a given observed SED and then see if the corresponding SFH and the AMR of this model are also able to reproduce the present time observational data of SFR and metallicity of the galaxy.

We show an example of this method in Fig. 3 where some SEDs from [6] of BCD galaxies are compared with the best model chosen for each one of them. In Fig. 4 we show the corresponding SFH and AMR with which the modeled SEDs were computed. The final values are within the error bars of observations for these same galaxies, compiled by the same authors [6]. Since each SED is well fitted and, simultaneously, the corresponding present–time data of the galaxy by the same

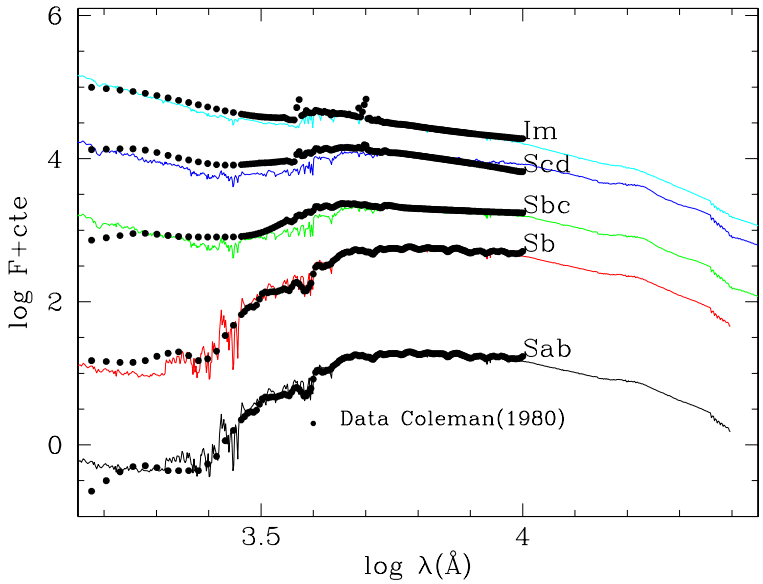

Fig. 2. The resulting spectral energy distributions obtained for models of Table 1 compared with the fiducial templates from [2].

chemical evolution model, we may be confident that these SFH and AMR give to us a reliable characterization of the evolutionary history of each galaxy.

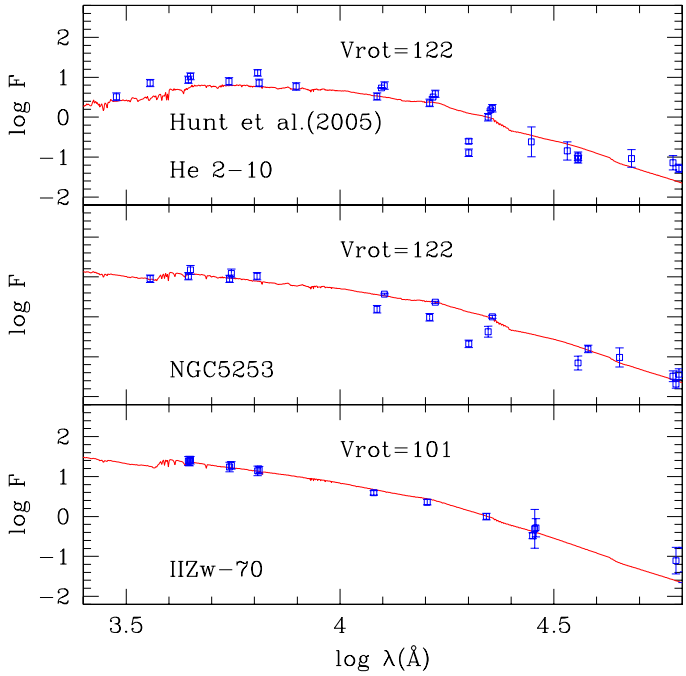

Fig. 3. The resulting spectral energy distributions –red solid lines- obtained to reproduce the observations from [6] –blue open squares- for three BCD galaxies.

4 Conclusions

We have computed a grid of 440 chemical evolution models for spiral and irregular galaxies of different sizes and masses (Vrot = 40–400 km.s^{-1}).

For each one of them we assumed 10 different SF efficiencies and the corresponding time evolutionary histories as given by the SFH and the AMR, were then used as inputs to obtain the SED through Eq.(1).

In this way we have obtained spectral energy distributions, colors, surface brightness and absorption spectral indices for each theoretical galaxy of the grid.

This combination of techniques allows the use of two data types: the ones proceeding from the gas phase as well as that coming from spectro-photometry. If a model is able to reproduce simultaneously both sets of observations for a given galaxy, the SFH and the AMR resulting from the corresponding chemical evolu-

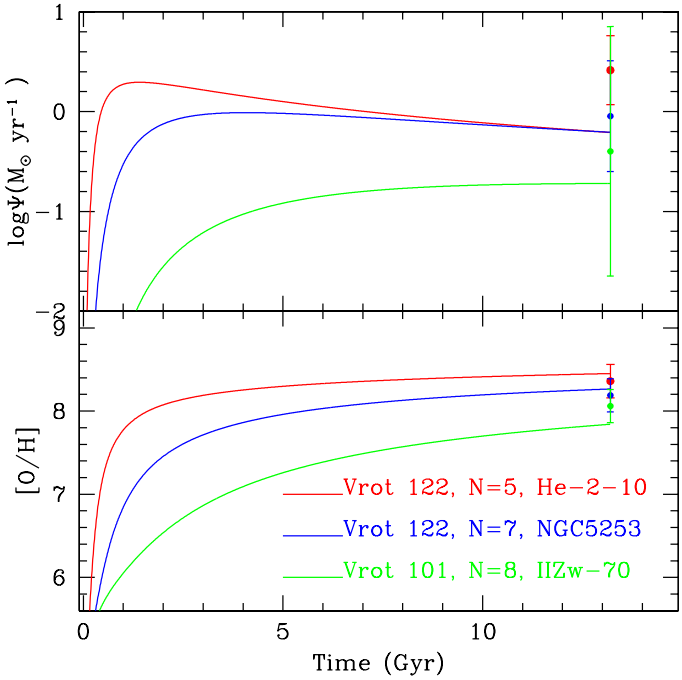

Fig. 4. The resulting SFH and AMR able to fit the SEDs of Fig. 3 represented by the blue, red and green lines for He-2-10, NGC5253 and IIZW-70, respectively. The present time data are shown in both panels by the full dots with error bars.

tion model may be considered sufficiently reliable to represent its very evolutionary history.

References

1. Cid Fernandes, R., Mateus, A., Sodré, L., Stasińska, G., & Gomes, J. M. 2005, MNRAS, 358, 363
2. Coleman, G. D., Wu, C.-C., & Weedman, D. W. 1980, ApJS, 43, 393
3. Ferrini, F., Matteucci, F., Pardi, C., & Penco, U. 1992, ApJ, 387, 138
4. Ferrini, F., Molla, M., Pardi, M. C., & Diaz, A. I. 1994, ApJ, 427, 745
5. Gónzalez- Delgado, R. M., Cerviño, M., Martins, L. P., Leitherer, C., & Hauschildt, P. H. 2005, MNRAS, 357, 945
6. Hunt, L., Bianchi, S., & Maiolino, R. 2005, A&A, 434, 849
7. Maraston, C. 2005, MNRAS, 362, 799
8. Mollá, M., & Díaz, A. I. 2005, MNRAS, 358, 521
9. Molla, M., Ferrini, F., & Diaz, A. I. 1996, ApJ, 466, 668
10. Mollá, M., & García-Vargas, M. L. 2000, A&A, 359, 18
11. Persic, M., Salucci, P., & Stel, F. 1996, MNRAS, 281, 27
12. Roberts, M. S., & Haynes, M. P. 1994, ARAA, 32, 115